Quantitative Accuracy of Slow-Rotating Dynamic SPECT

J. Zeintl, *Member, IEEE*, A. H. Vija, *Member, IEEE*, A. Yahil, *Member, IEEE*, J. Hornegger, *Member, IEEE*, and T. Kuwert

***Abstract*–We investigated biases in time-activity measurements relevant for quantitative dynamic SPECT/CT imaging when slow-rotating dual-headed gamma camera systems in combination with OSEM-3D (Flash3D) with scatter and attenuation correction are used. The goal was to assess the potential and also the limitations of clinical dual-headed SPECT/CT systems for the quantification of dynamic processes with focus on a renal time-activity function. We used simulations of a SPECT/CT system to estimate absolute quantitation errors in time-activity measurements. We systematically assessed dependencies of these errors on signal to noise ratio and sampling frequencies using a MAG-3 renal time-activity profile. In addition, a physical phantom was developed to measure dynamic processes on a clinical SPECT/CT system. The phantom consisted of a cylindrical chamber placed in a large cylinder phantom and connected to a programmable peristaltic pump. SPECT/CT acquisitions were performed by varying the rotation times of the SPECT system. Absolute activity concentrations were calculated by cross calibrating the imaging system with a well counter and using correction factors derived from simulations. Results from simulations show no significant differences in emission recovery coefficients within the range of 7.5 to 120 seconds per rotation. Phantom experiments using corrections from cross calibration and simulation show average estimation errors of -0.9% and -4.5% for 10 seconds and 60 seconds per rotation, respectively. Conclusion: We showed that quantitation of a renal dynamic process in phantoms using multiple time-contiguous SPECT acquisitions with 3D iterative reconstruction is possible with an accuracy of 4.5%.**

I. Introduction

In nuclear medicine clinical routine, dynamic processes such as renal function are commonly examined using planar dynamic scintigraphy [1, 2]. Disadvantages of planar data acquisitions include the overlap of target organs with other organs and approximative attenuation correction resulting in inaccurate quantitation. Several investigators [3-6] have tested SPECT imaging to overcome these limitations. These studies mainly focused on the correction of temporal inconsistencies of projection data in SPECT data using 4D image reconstruction. In the present study we investigate biases in time-activity measurements when slow-rotating dual-headed gamma camera systems in combination with co-registered CT images and OSEM-3D (Flash3D) with scatter and attenuation correction are used. The goal is to demonstrate the potential and the limitations of clinical dual-headed SPECT/CT systems for quantitative tomographic imaging of dynamic processes using multiple time-contiguous 3D acquisitions with 3D iterative reconstruction.

II. Material and Methods

We used both simulations of and measurements with a clinical SPECT/CT system (Symbia® T6) in this study.

Simulations were used to estimate the emission recovery coefficients for various imaging parameter settings of time-contiguous SPECT acquisitions. We used a quasi-analytical method (voxel size of the system model: 0.6 mm) and modeled the projection operator in 3D according to the detector and collimator specifications of the Symbia® series gamma cameras using low energy high resolution (LEHR) collimation. We accounted for photon attenuation in the object using a constant attenuation coefficient of 0.15 cm^{-1} and used a derived μ-map for attenuation correction. We assumed acquisitions with perfect scatter rejection of 140keV (Tc-99m) photons.

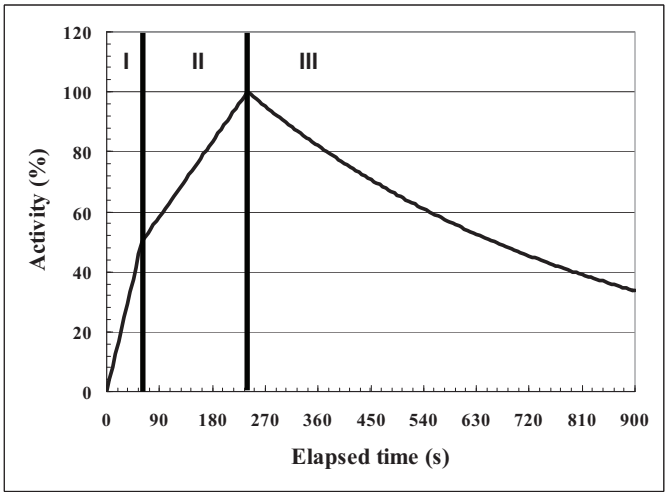

Fig. 1. Time-activity profile used for simulation of renal clearance. Three phases are modeled: Perfusion phase (I), secretion phase (II), and excretion phase (III).

Manuscript received November 13, 2009. *Asterisk indicates corresponding author.*

*Johannes Zeintl is a PhD student with the University of Erlangen-Nuremberg, Pattern Recognition Lab, Erlangen, Germany. (e-mail: Johannes.Zeintl@uk-erlangen.de).

A. Hans Vija is with Siemens Medical Solution USA, Inc., Molecular Imaging, Hoffman Estates, IL 60192, USA.

Amos Yahil is with Image Recon LLC, Stony Brook, NY, USA.

Joachim Hornegger is with the University of Erlangen-Nuremberg, Pattern Recognition Lab, Erlangen, Germany.

Torsten Kuwert is with the University of Erlangen-Nuremberg, Clinic of Nuclear Medicine.

We generated projections of a phantom with six spheres of varying diameters between 9.9 and 31.2 mm (Jaszczak Deluxe, Data Spectrum, Hillsborough, NC, USA). The activity concentration in the spheres changed over time according to a three-phase renal time-activity function with peak activity after four minutes (Fig. 1). The three phases modeled the perfusion phase (I), secretion phase (II), and excretion phase (III) [2]. The simulated SPECT acquisition used 60 views in a 180° rotation of two detectors (total angular range: 360°, total views: 120). Poisson noise was added to the generated projections. We varied signal to noise ratio and SPECT rotation times from $8x10^3$ to $128x10^3$ total peak counts and 7.5 seconds to 120 seconds per 180° rotation, respectively. For each parameter setting 5 independent realizations were generated. We used OSEM for image reconstruction including isotropic resolution recovery and attenuation correction.

Fig. 2 shows examples of reconstructed images from simulations using the time-activity profile from Fig. 1. In this example a maximum activity concentration of 0.08 µCi/ml at the peak of the time activity curve was used. We used a background activity concentration of 10% of the peak value in the target object.

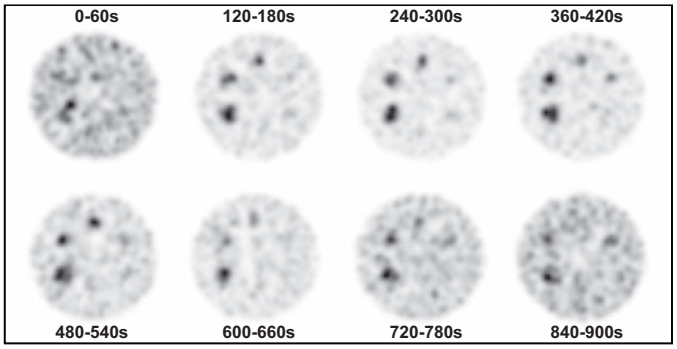

Fig. 2. Example reconstructed images of a simulated sphere phantom. Every second time frame is shown. Peak total counts per time frame were $64x10^3$.

In addition to simulations, a physical phantom for dynamic studies was developed. The phantom consisted of a cylindrical chamber (45.5 ml), connected to a programmable peristaltic pump (Cavro Scientific Instruments, Sunnyvale, CA, USA). The chamber was placed in a large water cylinder for imaging. Fig. 3 shows the setup of the pump and the cylindrical chamber with input and output tubing. Fig. 4 shows the imaging setup in the SPECT/CT system.

Dynamic SPECT/CT acquisitions were performed by varying the imaging speed of the SPECT system between 10s and 60s per 180° rotation with a fixed flow rate profile of the peristaltic pump as shown in Fig. 1. For attenuation correction a CT acquisition of the phantom was performed using 130kV, 30 mAs x-rays, and a smooth reconstruction kernel (B08s, Siemens Healthcare, Germany) with a 3 mm reconstruction increment. Images were reconstructed with OSEM-3D (Flash3D) with corrections for detector and collimator response, scatter, and attenuation. We used 16 iterations and 2 subsets without post-smoothing. Fig. 5 shows a reconstructed image of the phantom fused with the co-registered CT image.

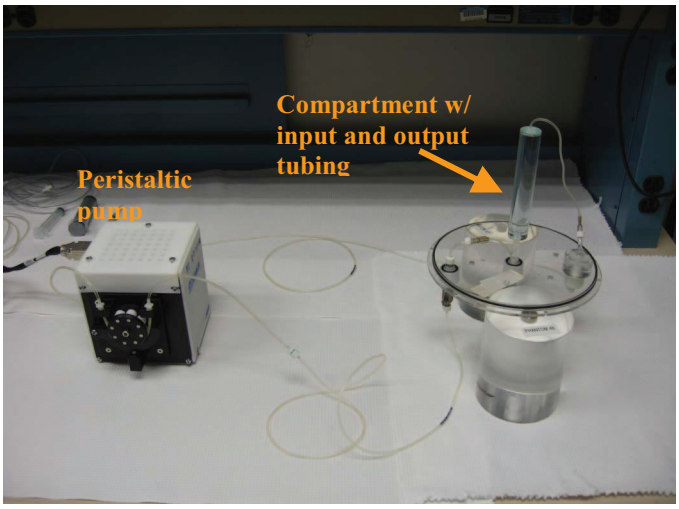

Fig. 3. Physical phantom for modeling dynamic processes. A cylindrical compartment was connected to a programmable peristaltic pump.

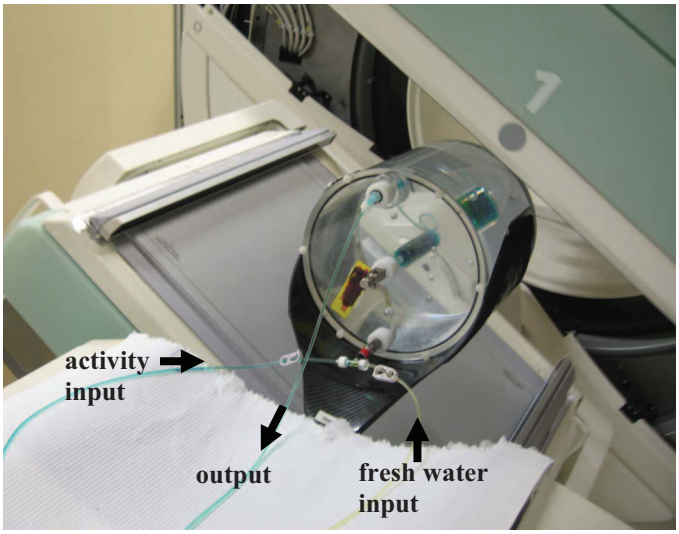

Fig. 4. Setup of the dynamic phantom in the dual headed SPECT/CT imaging system.

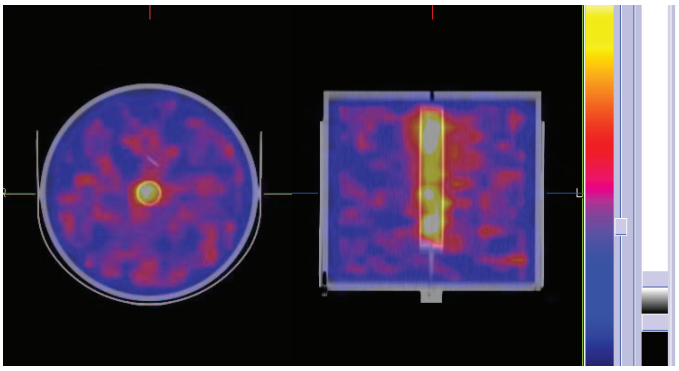
Fig. 5. Reconstructed image of the phantom fused with the co-registered CT image.

For quantitative evaluation we drew a volume of interest (VOI) in the reconstructed image using the boundaries of the registered CT image. We calculated the absolute activity concentration c_A using the following formula:

$$c_A = \frac{R / V_{VOI}}{S_{Vol}\ C_E(i)}, \qquad \text{Eq. 1}$$

where R is the average count rate in the drawn volume of interest, V_{VOI} the volume of the VOI, S_{Vol} the system volume sensitivity, and $C_E(i)$ the emission recovery coefficient at the specific imaging parameter set i. We derived the system volume sensitivity by cross calibrating the imaging system with the well counter. For this we performed a SPECT/CT acquisition using a large cylinder phantom (diameter: 21.6cm) filled with a known activity concentration $\hat{c}_A$ measured in the well counter. A large volume of interest (>3000ml) was drawn in the reconstructed image and S_{Vol} was calculated using the count rate per volume and the true activity concentration:

$$S_{Vol} = \frac{R / V_{VOI}}{\hat{c}_A}. \qquad \text{Eq. 2}$$

The emission recovery coefficient C_E was derived from simulations. We have shown previously that the emission recovery is highly dependent on object size and reconstruction parameters [7].

III. Results

Fig. 6 shows the mean emission recovery coefficients for the simulated sphere phantom. We used 16 iterations and 2 subsets for reconstruction without post-smoothing. Values are averaged over all time-contiguous acquisitions in a particular time-activity measurement. Fig. 7 gives the standard errors for the mean values in Fig. 6.

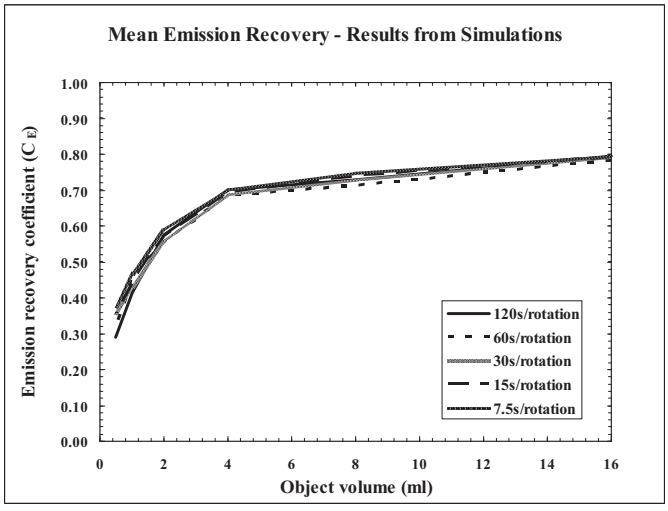

Fig. 6. Simulation results for the mean emission recovery coefficients for different object sizes and sampling frequencies.

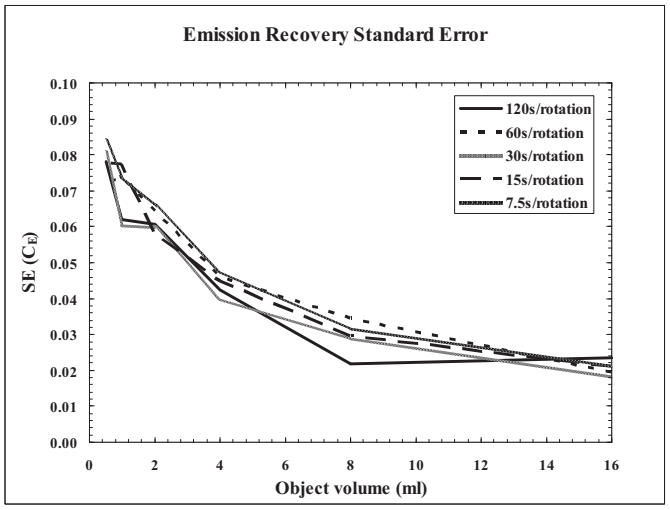

Fig. 7. Standard error of the mean emission recovery coefficients from Fig. 6 for different object sizes and sampling frequencies.

Fig. 8 to 11 show results from phantom experiments. True and calculated activity concentration of the renal process imaged with rotation times between 10s and 60s are shown. Error bars indicate the accumulated uncertainties due to measurement instrumentation such as well counter and pipette. Errors were propagated through the calibration procedure (Eq. 1 and Eq. 2). Gaps between the columns indicate acceleration and deceleration times of the imaging system in which no image data is taken. These times increase with detector rotation speed.

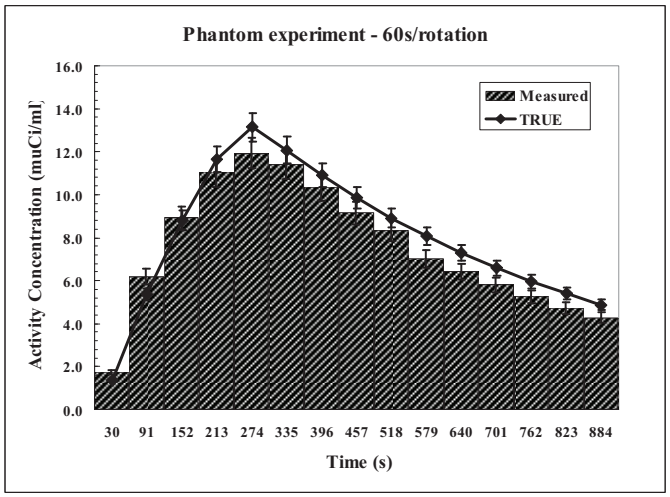

Fig. 8. True and calculated activity concentration of a renal process imaged in 60s time intervals.

In Table I the mean over all time-contiguous acquisitions in a particular measurement and the standard error of the difference between the true and the calculated activity concentration are shown. In addition, the estimation error of the area under the time activity curve is given.

The average accumulated uncertainty due to measurement instrumentation is 7.7%. The dominant factor in these uncertainties is the imprecision of the well counter which is

5% for Tc-99m (according to manufacturer's specification) after calibration using a standard reference source (Cs-137).

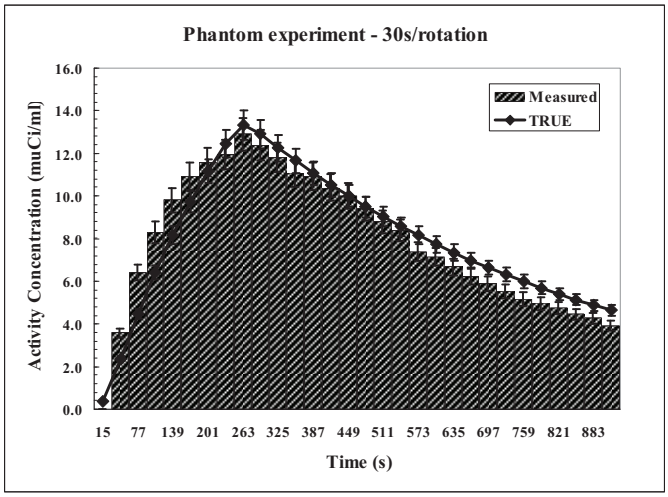

Fig. 9. True and calculated activity concentration of a renal process imaged in 30s time intervals.

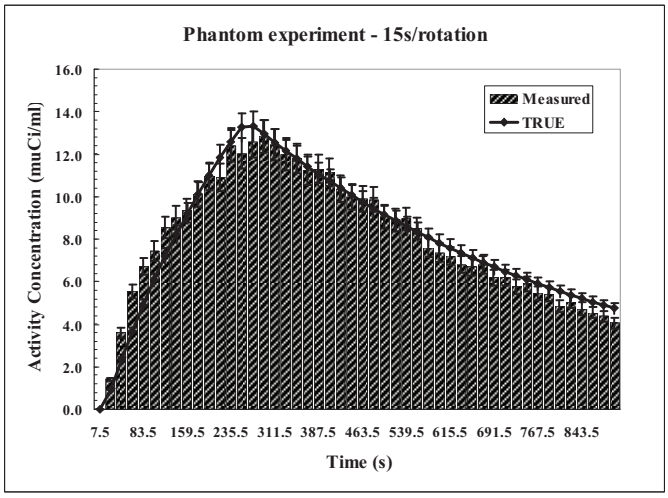

Fig. 10. True and calculated activity concentration of a renal process imaged in 15s time intervals.

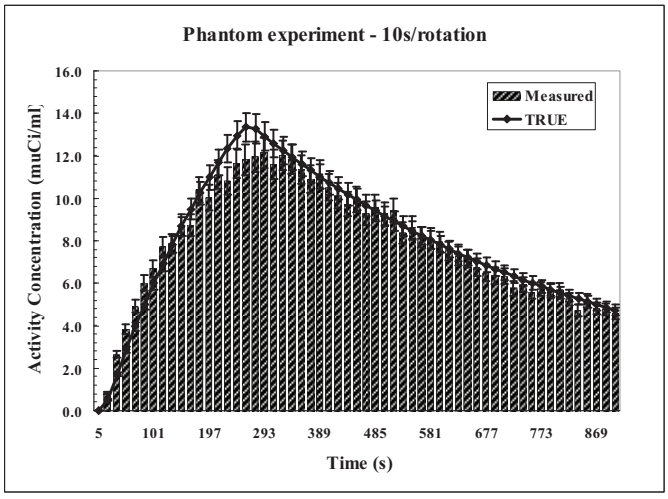

Fig. 11. True and calculated activity concentration of a renal process imaged in 10s time intervals.

TABLE I
RESULTS FROM PHANTOM EXPEXPERIMENTS WITH CALIBRATION ACCORDING TO EQUATION 1

Rotation time (s)	Difference - true vs. measured activity concentration		Mean uncertanties due to measurement instrumentation (SE)	Estimation error of area under the time activity curve
	Mean	SE of the mean		
60	-4.5%	3.0%	7.5%	-6.5%
30	-0.3%	3.0%	7.6%	1.5%
15	-1.0%	2.1%	7.8%	-0.6%
10	-0.9%	1.7%	8.0%	-2.1%

IV. DISCUSSION

Results from simulations indicate robust behavior of the emission recovery for the six tested object sizes against changes in sampling frequencies and noise levels. Note that the method used to simulate the imaging system only takes the primary photons of 140 keV into account, neglecting septal penetration and assuming perfect scatter rejection. Furthermore, object boundaries need to be known precisely to draw correct regions of interest. In practice, this postulates co-registered SPECT/CT imaging.

Phantom studies show an underestimation of the activity concentration of 0.3%-4.5% when the proposed calibration method is applied. Further analysis needs to be done to investigate this systematic bias.

Object and collimator scatter is present in the acquired data and corrected using the standard techniques provided by the reconstruction software package. We used correction factors from simulations for the calibration of the imaging system and therefore introduced uncertainties regarding the treatment of scatter and septal penetration which were not accounted for in this work.

In our study the dominant factor in the accumulated uncertainties due to measurement instrumentation is the well counter (5%). Using high precision measurement tools the overall uncertainties can be minimized. Still, in a clinical setup, using standard measurement tools, the presented uncertainty values are realistic.

V. CONCLUSION

We could show that absolute quantitation of a renal dynamic process in phantoms using multiple time-contiguous SPECT acquisitions with 3D iterative reconstruction is possible within 4.5% accuracy if the target object boundaries are known. The cumulative uncertainties due to measurement instrumentation (e.g. well counter, pipette, etc.) are between 7.5% and 8.0% using standard measurement tools. Additional work will be done to study the impact of faster activity flow rates, rotation times, and different orbit types on the quantitation accuracy.

ACKNOWLEDGMENTS

The authors would like to thank Ron Malmin and Manojeet Bhattacharya for valuable discussions and the Systems Test team at Hoffman Estates for their help during system quality control and acquisition of the data.

REFERENCES

[1] G. N. Sfakianakis, E. Sfakianaki, M. Georgiou *et al.*, "A renal protocol for all ages and all indications: Mercapto-Acetyl-Triglycine (MAG3) with simultaneous injection of Furosemide (MAG3-F0): A 17-year experience," *Semin Nucl Med,* vol. 39, pp. 156-173, 2009.

[2] T. Zajic, and E. Moser, "Procedure guidelines for dynamic renal scintigraphy," *NuklearMedizin,* vol. 43, pp. 177-80, 2004.

[3] T. Farncombe, A. Celler, D. Noll *et al.*, "Dynamic SPECT imaging using a single camera rotation (dSPECT)," *Nuclear Science, IEEE Transactions on,* vol. 46, no. 4, pp. 1055-1061, 1999.

[4] T. Farncombe, M. King, A. Celler *et al.*, "A fully 4d expectation maximization algorithm using gaussian diffusion based detector response for slow camera rotation dynamic SPECT," *Proceedings of the 2001 International Meeting on Fully 3D Image Reconstruction in Radiology and Nuclear Medicine*, 2001.

[5] D. J. Kadrmas, E. V. R. DiBella, R. H. Huesman *et al.*, "Analytical propagation of errors in dynamic SPECT: Estimators, degrading factors, bias and noise," *Physics in Medicine and Biology,* vol. 44, no. 8, pp. 1997-2014, 1999.

[6] A. Sitek, G. T. Gullberg, E. V. R. Di Bella *et al.*, "Reconstruction of Dynamic Renal Tomographic Data Acquired by Slow Rotation," *J Nucl Med,* vol. 42, no. 11, pp. 1704-1712, November 1, 2001, 2001.

[7] J. Zeintl, A. H. Vija, A. Yahil *et al.*, "Towards quantitative SPECT: Error estimation of SPECT OSEM with 3D resolution recovery, attenuation correction and scatter correction." pp. 4106-4111.